

# Root-aligned SMILES for Molecular Retrosynthesis Prediction

Zipeng Zhong<sup>1</sup>, Jie Song<sup>2</sup>, Zunlei Feng<sup>2</sup>, Tiantao Liu<sup>3</sup>, Lingxiang Jia<sup>1</sup>, Shaolun Yao<sup>1</sup>, Min Wu<sup>4</sup>, Tingjun Hou<sup>3\*</sup> and Mingli Song<sup>1\*</sup>

<sup>1</sup>College of Computer Science and Technology, Zhejiang University, 310027, Zhejiang, P.R. China.

<sup>2</sup>School of Software Technology, Zhejiang University, 315048, Zhejiang, P.R. China.

<sup>3</sup>Innovation Institute for Artificial Intelligence in Medicine of Zhejiang University, College of Pharmaceutical Sciences, Zhejiang University, 310058, Zhejiang, P.R. China.

<sup>4</sup> Hangzhou Huadong Medicine Group Pharmaceutical Research Institute, 310011, Zhejiang, P.R. China.

\*Corresponding author(s). E-mail(s): [tingjunhou@zju.edu.cn](mailto:tingjunhou@zju.edu.cn); [brooksong@zju.edu.cn](mailto:brooksong@zju.edu.cn);  
Contributing authors: [zipengzhong@zju.edu.cn](mailto:zipengzhong@zju.edu.cn); [sjie@zju.edu.cn](mailto:sjie@zju.edu.cn); [zunleifeng@zju.edu.cn](mailto:zunleifeng@zju.edu.cn);  
[liutiant@zju.edu.cn](mailto:liutiant@zju.edu.cn); [lingxiangjia@zju.edu.cn](mailto:lingxiangjia@zju.edu.cn); [yaoshaolun@zju.edu.cn](mailto:yaoshaolun@zju.edu.cn);  
[swgcwumin@hdnewdrug.com](mailto:swgcwumin@hdnewdrug.com);

Retrosynthesis prediction is a fundamental problem in organic synthesis, where the task is to discover precursor molecules that can be used to synthesize a target molecule. A popular paradigm of existing computational retrosynthesis methods formulate retrosynthesis prediction as a sequence-to-sequence translation problem, where the typical SMILES representations are adopted for both reactants and products. However, the general-purpose SMILES neglects the characteristics of retrosynthesis that 1) the search space of the reactants is quite huge, and 2) the molecular graph topology is largely unaltered from products to reactants, resulting in the suboptimal performance of SMILES if straightforwardly applied. In this article, we propose the root-aligned SMILES (R-SMILES), which specifies a tightly aligned one-to-one mapping between the product and the reactant SMILES, to narrow the string representation discrepancy for more efficient retrosynthesis. As the minimum edit distance between the input and the output is significantly decreased with the proposed R-SMILES, the computational model is largely relieved from learning the complex syntax and dedicated to learning the chemical knowledge for retrosynthesis. We compare the proposed R-SMILES with various state-of-the-art baselines on different benchmarks and show that it significantly outperforms them all, demonstrating the superiority of the proposed method.

**Keywords:** retrosynthesis, SMILES, transformer

As a fundamental problem of organic chemistry, organic synthesis plays a vital role in drug discovery and material design. Retrosynthesis [1, 2], which aims at designing reaction pathways and intermediates for a target compound, is an important technique for solving the planning of organic

synthesis. Retrosynthesis is challenging as the search space of all possible transformations is huge by nature. In the early days, expert synthetic chemists could convert target molecules to simpler precursor molecules with their familiar reactions. To integrate more chemical knowledge and be

more efficient, the first computer-aided synthesis planning program LHASA [3] was formally proposed by Corey et al. and showed great potential. Since then, many rule-based organic synthesis systems have come out, such as SYNLMA [4], WODCA [5], and Synthia [6]. However, with the increase of chemical reaction rules, the cost of manually hard-coding chemical rules into computer systems is getting higher. Alternatively, people have begun to explore fully data-driven retrosynthesis approaches, where the current literature can be roughly categorized into two schools: selection-based methods [7–12] and generation-based methods [13–24]. Selection-based methods turn retrosynthesis into a ranking or classification problem, where the goal is to rank the matched reaction templates [7–10] or reactants [11, 12] higher than those unmatched for the target molecule. Despite encouraging results achieved, selection-based methods not only require expensive computation but also suffer from poor generalization on new target structures and reaction types. Generation-based methods, however, address the retrosynthesis problem with a generative model (*e.g.*, transformers [14–21] or GNNs [22–24]) where reactants are generated rather than selected, which significantly alleviates the poor generalization issue of selection-based methods.

Before applying generation-based methods for retrosynthesis, the first and critical step is to select the appropriate representation forms of both the product and the reactants. Two types of molecular representations are most widely used currently, including molecular graphs and string sequences. A molecular graph explicitly describes the topological structure of the molecule, upon which the recently well-developed GNNs [25, 26] can be directly leveraged. However, graph-based representations involve a graph generation problem in retrosynthesis, which is challenging and usually solved by sequential graph edit operation predictions [22–24]. In contrast, another popular paradigm to represent molecules is using strings that are generated following some predefined chemical notation systems, of which the simplified molecular-input line-entry system (SMILES) [27] is most widely used currently. With string sequences as the representations of molecules, retrosynthesis can be reformulated as the typical seq2seq translation problem in NLP, where plenty of methods or models can be borrowed.

SMILES has been widely used for retrosynthesis predictions [14–21] in the current literature. However, in this work we argue that the general-purpose SMILES is deficient for the retrosynthesis problem. Since SMILES is generated by a depth-first traversal of the molecular graph, a molecule can have multiple valid SMILES representations by selecting different root atoms as the starting nodes of traversal. The one-to-many mappings between molecules and SMILES turn retrosynthesis into a one-to-many<sup>1</sup> mapping problem between products and reactants, which renders retrosynthesis extremely challenging as the computational model should learn not only the chemical rules for retrosynthesis but also the SMILES syntax for SMILES string validity. Several canonicalization methods [28, 29] can be adopted to generate canonical SMILES that ensures a one-to-one mapping between molecules and SMILES. However, these methods are designed for each individual molecule without considering the relationship between product and reactant molecules, which leads to the large input-output (or product-reactant) SMILES discrepancy, as shown by the two examples (2,2,2-trichloroethyl prop-2-enoate and 2-ethyl-6-methylpyridine-3-carbonitrile) in Fig 1. The large input-output SMILES discrepancy leaves the search space of reactants huge, degrading the performance of retrosynthesis models. Moreover, the canonical SMILES is incompatible with some data augmentation techniques where multiple SMILES are needed for one molecule to bypass the data scarcity issue, as the concept of “canonical SMILES” is violated by multiple SMILES for one molecule.

In contrast to the large edit distance between the input and the output SMILES adopted in existing models, the molecular graph topology is in fact largely unaltered from reactants to products as the molecular changes usually occur locally during the chemical reactions [10]. In this article, we propose the root-aligned SMILES (R-SMILES) for more efficient retrosynthesis. As shown in Fig 1, for each chemical reaction, R-SMILES adopts the same atom as the root (*i.e.*, the starting atom) of the SMILES strings for both the products and the reactants, which makes the input and

---

<sup>1</sup>For a given input SMILES, there can be multiple correct output SMILES.

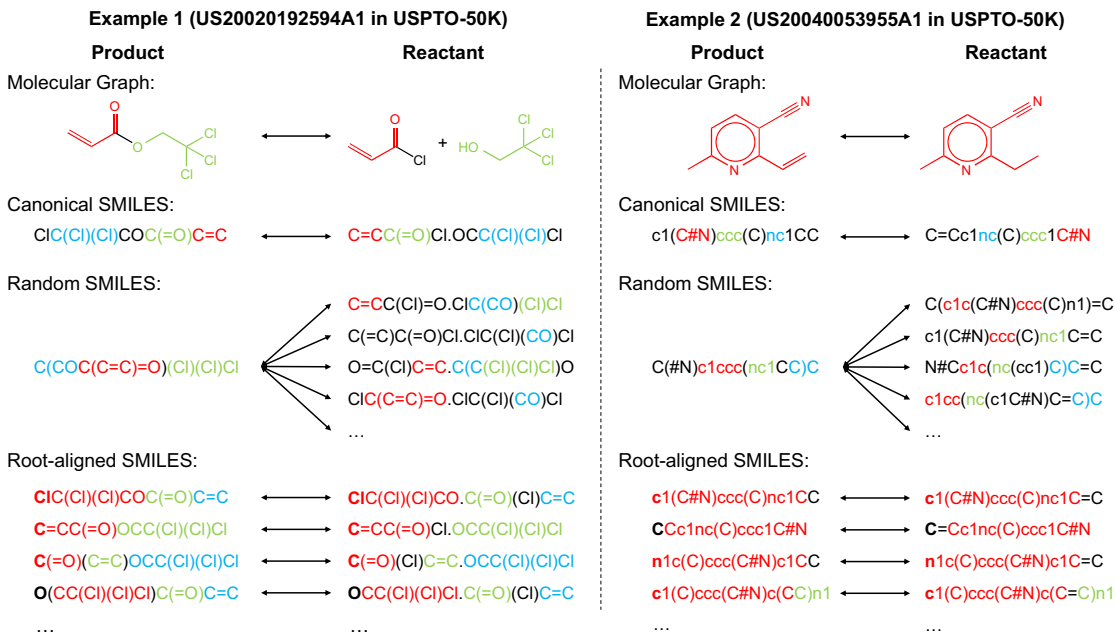


**Fig. 1 Comparison of differences between input and output for different molecular representations.** The root atom of root-aligned SMILES is bold. The common structures that contain at least two atoms of input and output are represented with the same color. The more colored fragments in the output, the more similar they are.

the output SMILES maintain a one-to-one mapping and highly similar to each other. The high similarity between the input and output makes retrosynthesis with R-SMILES very close to the typical autoencoding problem [30, 31] where the goal is to learn an identity mapping between the input and the output, with some bottleneck features summarizing the most important aspects in the data. Motivated by this, we propose a transformer-based autoencoder for retrosynthesis. With the proposed R-SMILES, we first pretrain the proposed autoencoder with the cheaply available unlabeled molecular data for extracting the compact molecular representations and mastering essential SMILES syntax in the decoder. Then the model is finetuned with the reaction data, where the model is largely relieved from learning the complex syntax and can be dedicated to learning the chemical knowledge for retrosynthesis. We conducted extensive experiments to validate the proposed method, with template-free (*i.e.*, learning a direct mapping from the product to reactants [13–16, 19–21, 24, 32]) and semi-template (*i.e.*, first identifying intermediate molecules called synthons, and then completing synthons into reactants [17, 18, 22, 23]) variants. Compared with

other baselines, the proposed template-free and semi-template variants yield significantly superior performance on both USPTO-50K and USPTO-FULL datasets. For a better understanding of the proposed method, we visualize the cross-attention mechanism in transformer with R-SMILES and show some interesting aspects of our results. Furthermore, we provide several multistep retrosynthesis examples successfully predicted by our method, which illustrates its great potential in complicated retrosynthesis tasks.

## Results and discussion

To thoroughly evaluate the performance of the R-SMILES and the autoencoder proposed for retrosynthesis, we implement our method with both template-free and semi-template variants to make comparisons with more SOTA methods. Template-free methods [13–16, 19–21, 24, 32] learn a direct mapping from products to reactants. Here for simplicity, the product is abbreviated as P and the reactant as R. The transformation from products to reactants in template-free methods is denoted by P2R. Semi-template methods [17, 18, 22, 23] decompose retrosynthesis into two stages:

1) first identify intermediate molecules called synthons, and then 2) complete synthons into reactants. We use S to represent synthons, and P2S and S2R to represent the two stages, respectively. The template-free variant is an end-to-end seq2seq model taking R-SMILES as the input and output. As for the semi-template variant, we also formulate S2R as a seq2seq problem and use the proposed autoencoder with R-SMILES to solve it. However, P2S is more suitable to be formulated as a graph link prediction problem, and thus we adopt a GNN model here for superior overall performance. A detailed description of the adopted GNN can be found in Section Methods. In addition, many existing works [9, 10, 22–24] demonstrate their performances with the reaction type known for each product. Since the reaction type is not always available in real-world scenarios, all experiments in this work are carried out without this information.

**Dataset Summary.** Experiments are conducted on USPTO-50K [33] and USPTO-FULL [9], both of which are widely used as public benchmarking datasets for the retrosynthesis task. USPTO-50K is a high-quality dataset containing about 50,000 reactions with accurate atom mappings between products and reactants. USPTO-FULL, the superset of USPTO-50K, is derived from USPTO 1976-2016. It is a much larger dataset for chemical reactions, consisting of about 1,000,000 reactions. Reactions that contain multiple products are duplicated into multiple reactions to ensure that every reaction in data has only one product. Invalid data that contains no products or just a single ion as reactants are removed. After these preprocessing steps, we can get a clean version of USPTO-FULL dataset.

**Statistical analysis of the minimum edit distance with R-SMILES.** We first provide some statistical analysis of the minimum edit distance between the input and the output with the proposed R-SMILES. The minimum edit distance between two strings is defined as the minimum number of editing operations (including insertion, deletion, and substitution) needed to transform one into the other. Here we adopt it to measure the discrepancy between input and output SMILES. With canonical SMILES, the average minimum edit distance between the product and the reactant is 17.9 on USPTO-50K and 19.8 on USPTO-FULL. With the proposed R-SMILES,

the minimum edit distances become 14.1 and 16.6, decreasing by 21% and 16%, respectively. Moreover, to alleviate the overfitting problem, data augmentation is critical and widely used in existing methods [18–20]. However, with the randomized SMILES as used in most existing works, the minimum edit distance will be significantly increased. For example, with 5× augmentation, the minimum edit distance is increased to 28.4 on USPTO-50K, which is more than two times of that of the proposed R-SMILES (14.1) where the minimum edit distance of R-SMILES keeps unchanged with data augmentation. The larger discrepancy and one-to-many mapping of randomized SMILES make the learning problem more difficult, degrading the model performance of retrosynthesis prediction. For more detailed statistics, please refer to Supplementary Table. 2.

**Comparisons with SOTA retrosynthesis methods.** We make comparisons between the proposed method and existing SOTA competitors, including selection-based (*i.e.*, template-based) and generation-based (including template-free and semi-template) methods. We adopt the exact match accuracy and the maximal fragment accuracy [19] as the metrics to evaluate the performance. Exact match accuracy that is widely used as the metric of the retrosynthesis performance, represents the percentage of predicted reactants that are identical to the ground truth. The maximal fragment accuracy, inspired by classical retrosynthesis, requires the exact match of only the largest reactant. We use the top-K exact match accuracy as the main metric to report the performance. The maximal fragment accuracy is adopted in some cases for a more comprehensive comparison. Experiments are conducted on both USPTO-50K and USPTO-FULL. Results are shown in Table 1.

From the results, we make the following three main conclusions. (1) Generally speaking, the proposed methods, including the semi-template and the template-free variants, consistently outperform SOTA competitors by a large margin. For example, on USPTO-50K the proposed template-free variant outperforms the current best method by absolute 6.2% and 3.5% in top-10 and top-50 exact match accuracy, respectively. On the more challenging USPTO-FULL dataset, the accuracy improvement is still very substantial, by 1.6% in top-1, 2.7% in top-10, and 8.3% in top-50. These

**Table 1** Top-K results on USPTO-50K (**top**) and USPTO-FULL (**bottom**) datasets. Unless specially specified, the results are reported in exact match accuracy. Symbol † denotes that the maximal fragment accuracy is reported. Symbol \* denotes that the result is implemented by the open-source code with well-tuned hyperparameters. SEMI and FREE denote our semi-template and template-free variants, respectively.

USPTO-50K top-K Accuracy (%)								
Category	Model	Year	K = 1	3	5	10	20	50
Template-Based	retrosim [7]	2017	37.3	54.7	63.3	74.1	82.0	85.3
	neuralsym [8]	2017	44.4	6.3	72.4	78.9	82.2	83.1
	GLN [9]	2019	52.5	69.0	75.6	83.7	89.0	92.4
	LocalRetro [10]	2021	53.4	77.5	85.9	92.4	-	97.7
Semi-template	G2Gs [22]	2020	48.9	67.6	72.5	75.5	-	-
	GraphRetro [23]	2021	53.7	68.3	72.2	75.5	-	-
	RetroXpert [17]	2020	50.4	61.1	62.3	63.4	63.9	64.0
	RetroPrime [18]	2021	51.4	70.8	74.0	76.1	-	-
	Ours (SEMI)	2022	<b>59.0 (±0.36)</b>	<b>75.4 (±0.19)</b>	<b>78.2 (±0.15)</b>	<b>80.1 (±0.38)</b>	-	-
Template-Free	Liu’s Seq2seq [13]	2017	37.4	52.4	57.0	61.7	65.9	70.7
	GTA [20]	2021	51.1 (±0.29)	67.6 (±0.22)	74.8 (±0.36)	81.6 (±0.22)	-	-
	Dual-TF [32]	2021	53.3	69.7	73.0	75.0	-	-
	MEGAN [24]	2021	48.1	70.7	78.4	86.1	90.3	93.2
	Tied Transformer [21]	2021	47.1	67.2	73.5	78.5	-	-
	AT [19]	2020	53.5	-	81.0	85.7	-	-
	Ours (FREE)	2022	<b>55.0 (±0.08)</b>	<b>78.8 (±0.23)</b>	<b>86.5 (±0.25)</b>	<b>92.3 (±0.46)</b>	<b>95.3 (±0.48)</b>	<b>96.7 (±0.56)</b>
	MEGAN† [24]	2021	54.2	75.7	83.1	89.2	92.7	95.1
	Tied Transformer† [21]	2021	51.8	72.5	78.2	82.4	-	-
	AT† [19]	2020	58.5	-	85.4	90.0	-	-
Ours (FREE)†	2022	<b>59.7 (±0.08)</b>	<b>81.7 (±0.16)</b>	<b>88.4 (±0.30)</b>	<b>93.7 (±0.31)</b>	<b>96.2 (±0.38)</b>	<b>97.3 (±0.51)</b>	
USPTO-FULL top-K Accuracy (%)								
Category	Model	Year	K = 1	3	5	10	20	50
Template-Based	retrosim [7]	2017	32.8	-	-	56.1	-	-
	neuralsym [8]	2017	35.8	-	-	60.8	-	-
	GLN [9]	2019	39.3	-	-	63.7	-	-
	LocalRetro* [10]	2021	39.1	53.3	58.4	63.7	67.5	70.7
Semi-template	RetroPrime [18]	2021	44.1	-	-	68.5	-	-
	Ours (SEMI)	2022	<b>45.2(±0.28)</b>	-	-	<b>70.2(±0.37)</b>	-	-
Template-Free	MEGAN [24]	2020	33.6	-	-	63.9	-	74.1
	GTA [20]	2021	46.6 (±0.20)	-	-	70.4 (±0.15)	-	-
	AT [19]	2020	46.2	-	-	73.3	-	-
	Ours (FREE)	2022	<b>47.7 (±0.08)</b>	<b>64.1 (±0.08)</b>	<b>70.0 (±0.06)</b>	<b>76.0 (±0.05)</b>	<b>78.1 (±0.05)</b>	<b>82.4 (±0.04)</b>

impressing and consistent results demonstrate the superiority of the proposed methods over SOTA methods. (2) The template-free variant outperforms the semi-template variant in most cases, for example, by 8.3% and 12.2% in top-5 and top-10, respectively in exact match accuracy on USPTO-50K. The main factor accounting for this phenomenon lies in the two stages of semi-template methods, where P2S usually makes noisy predictions that can hardly be rectified by the following S2R model. The end-to-end template-free variant bypasses this issue and thus yields superior performance. (3) The template-free variant achieves superior or at least comparable performance to the current SOTA template-based method LocalRetro [10] on USPTO-50K. However, as template-based approaches are well known to be poor at generalizing to new reaction templates, the performance

of LocalRetro on the more challenging USPTO-FULL dataset is substantially worse than the proposed template-free variant. All these results verify the effectiveness and the superiority of our proposed method.

**Superiority of the proposed R-SMILES with data augmentation.** Here we evaluate the superiority of the proposed R-SMILES in retrosynthesis. We adopt the vanilla transformer [34], a popular language translation model, as the retrosynthesis model. In retrosynthesis, data augmentation can be applied to both the training and the test data [19], or only one of them. To test the performance of R-SMILES with data augmentation, different times of augmentation are conducted on training and test data. Here we take the widely used canonical SMILES as the baseline for comparisons. Experiments are conducted on

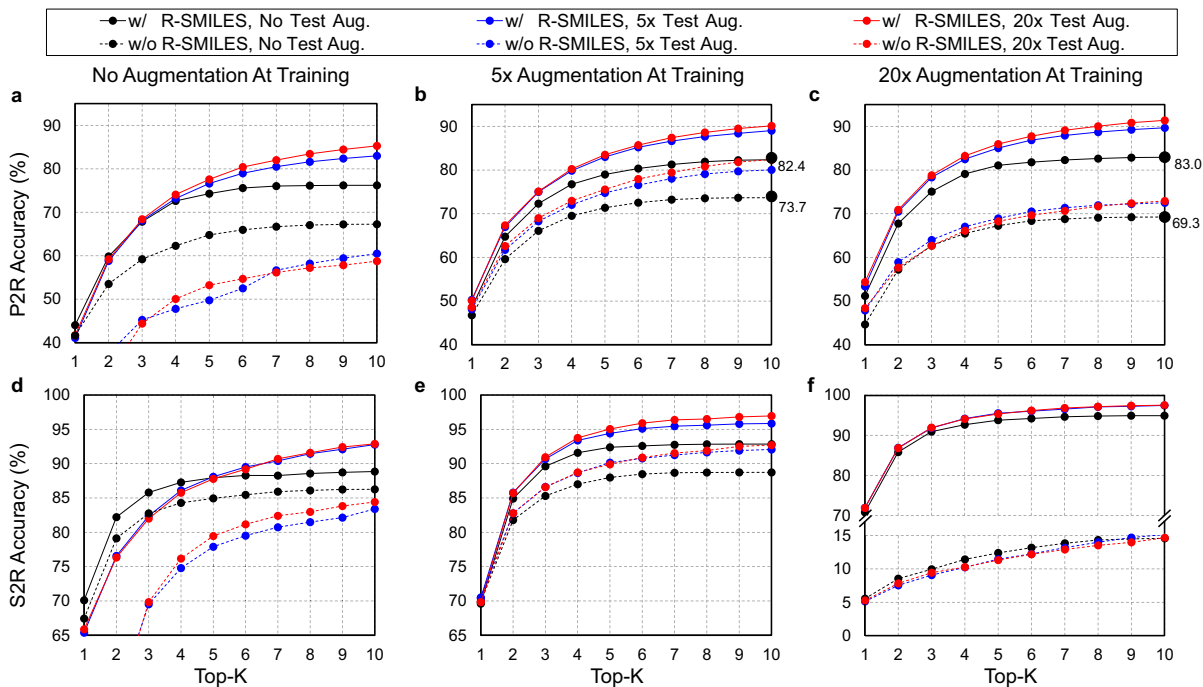


**Fig. 2** Top-K accuracy (%) with/without R-SMILES on USPTO-50K for P2R (a, b, c) and S2R (d, e, f). The solid lines (w/ R-SMILES) and dashed lines (w/o R-SMILES) represent the performance with or without R-SMILES, respectively. The lines with different colors represent the performance in different test set augmentation scenarios.

the USPTO-50K dataset, with both the template-free (P2R) and the semi-template (S2R) variants. Results are shown in Fig. 2. In each subplot, the solid and dashed lines represent the performance with and without (*i.e.*, with canonical SMILES) R-SMILES, and different colors represent times of data augmentation. First of all, it is evident that the solid lines are consistently above the dashed lines in the same color, which reveals that the performance with R-SMILES is consistently superior to the widely used canonical SMILES in the same data augmentation scenario. An interesting observation is that if no training data augmentation is applied (Fig. 2a, d), doing augmentation on the test data will lower the performance with the canonical SMILES. However, with the proposed R-SMILES, the accuracy is improved as expected. It indicates that the proposed method is more compatible with test data augmentation even though augmentation is not applied at the training time. Finally, by making plot-level comparisons, we can find that with more training data augmentation, the proposed R-SMILES yield higher accuracy. For example, if no data augmentation is applied at test time, 5x data

augmentation yields 82.4% top-10 accuracy, while 20x augmentation achieves 83.0%. However, the canonical SMILES may yield inferior performance if too much training data augmentation is applied. Under the same situation as an example above, 5x data augmentation with canonical SMILES yields 73.7% top-10 accuracy, while 20x augmentation achieves only 69.3%. The underlying reason is that if too much training data augmentation is applied, the retrosynthesis task becomes a one-to-many problem, which is extremely difficult for the model to learn useful chemical knowledge for retrosynthesis. On the other hand, if no training data augmentation is used, the model may suffer from the overfitting problem, which leaves a trade-off issue regarding the data augmentation with the canonical SMILES. However, the proposed R-SMILES perfectly solves this problem and can reliably enjoy the higher performance with more data augmentation.

**Visualization of cross-attention mechanism in transformer with R-SMILES.** To further illustrate how transformer works with R-SMILES, we display a retrosynthesis example of 3-oxo-4H-1,4-benzothiazine-6-carboxylic acid, where a

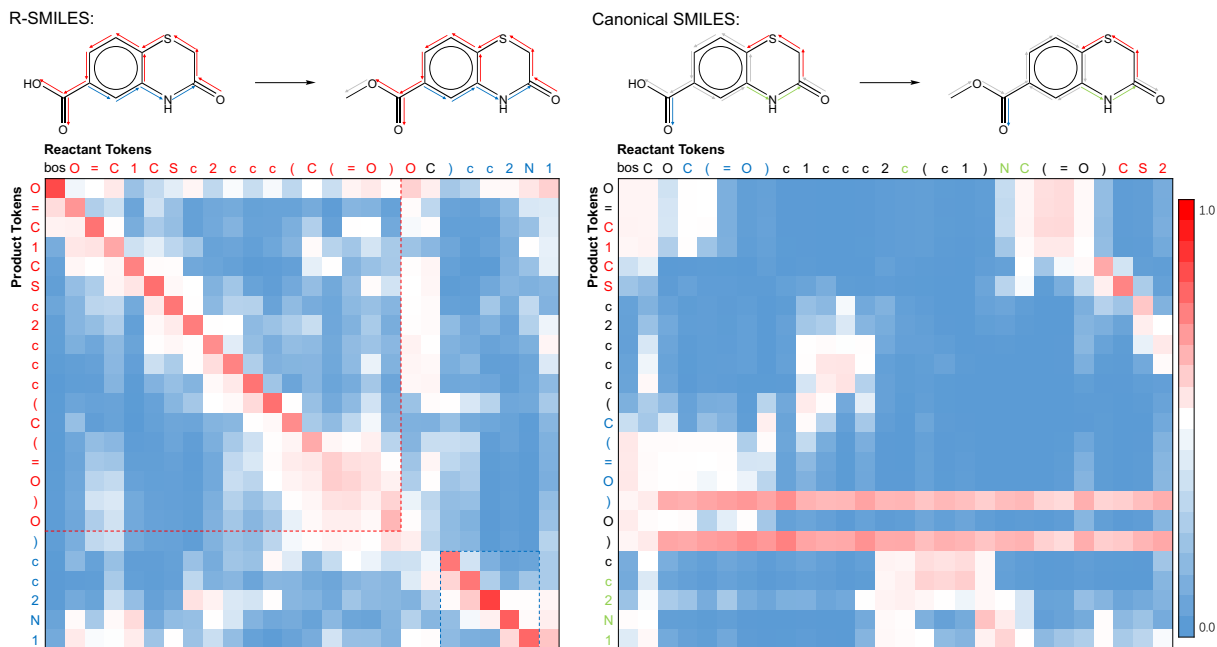


**Fig. 3 Visualization of the cross attention with the proposed R-SMILES (Left) and the canonical SMILES (Right).** This is an example of the retrosynthesis of 3-oxo-4H-1,4-benzothiazine-6-carboxylic acid that is taken from our test set of USPTO-50K (id: US20100081650A1). **Top:** the molecular graphs of products and reactants. **Bottom:** the cross attention map between product and reactant tokens. Arrows in the molecular graphs represent the atomic traversal order of the SMILES. The arrows with the same traversal order in the products and the reactants are marked with the same color as well as their corresponding SMILES tokens. The gray arrows in reactant graphs represent the absence of the corresponding arrows. Each column in the attention map represents the attention over the product tokens for predicting the next reactant token. The “bos” token is the beginning of reactant tokens and will be removed after the decoding process completes.

new carbon atom is added to the reactant. The visualization of the cross-attention between the product and the reactant tokens is shown in Fig. 3. The adopted transformer is an autoregressive model, where the last predicted token is taken as input for predicting the next token. The cross-attention represents the correlation between reactant tokens and product tokens. Since the proposed R-SMILES makes the reactant SMILES tightly aligned to the product SMILES, as shown by the arrows in molecular graphs in the left subplot of Fig. 3, the prediction of the reactant tokens can be largely based on input tokens, with nearly the same token order. It is verified by the clear strong correlation between nearly diagonally paired tokens as shown in the rectangular dashed red box. However, when it comes to the reaction center (*i.e.*, the new carbon atom), the attention becomes more evenly distributed, as shown by the attention of the new atom “C” in this

example. After the reaction center, the prediction of the reactant tokens can be again largely dependent on the corresponding tokens in the product tokens, as indicated by the rectangular dashed blue box. However, for canonical SMILES, as reactant tokens and product tokens are mostly unaligned, the model should learn to master the complex syntax, and thus the performance on retrosynthesis is largely affected. It is revealed by the cross-attention between the product and the reactant tokens as shown in the right subplot in Fig 3, where the results are much harder to understand for us.

**Discussion of R-SMILES in more aspects.** Here we conduct further studies to shed more light on the proposed R-SMILES. Specifically, we investigate the performance of R-SMILES with some more complex reactions in the USPTO-50K, including reactions involving many new atoms in the reactants and chirality.

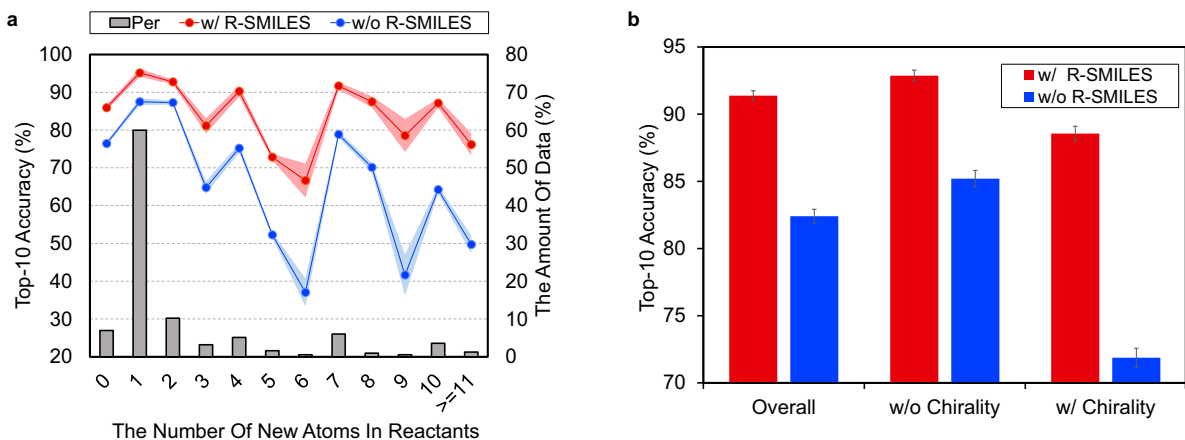


**Fig. 4 Accuracies for complex reactions.** **a**, Top-10 accuracy according to the number of new atoms in reactants. The red and blue lines represent the performance with/without R-SMILES. The gray bar means the percentage of this kind of reaction in the test set. **b**, Top-10 accuracy for reactions involving with/without chirality. The red and blue bars represent the performance with or without R-SMILES.

*The number of new atoms in reactants.* According to the number of new atoms (hydrogen atoms do not count) in reactants, we illustrate top-10 accuracy with or without R-SMILES and the amount of data in Fig. 4a. Similar to the previous results, the red line is always above the blue line, illustrating that the performance with R-SMILES surpasses the other by a large margin. In addition, the more new atoms in reactants, the larger improvement, especially for the situations with small amounts of data. For the reactions whose numbers of new atoms are 9, the improvement is impressively 39.3%, demonstrating that R-SMILES remains robust even with small amounts of data. This is because with R-SMILES that reduces the differences between the input and the output SMILES, the model can pay attention to the new fragments in the output SMILES.

*Chirality.* Chirality is a property of asymmetry and is important in drug discovery and stereochemistry. It can be represented by '@' or '@@' in SMILES sequences. We count 851 reactions with chirality in our test set of USPTO-50K and exhibit the top-10 accuracy with or without chirality and overall accuracy in Fig. 4b. When chirality exists in the reaction, the accuracy without R-SMILES drops 13.3%. In comparison, ours drops only 4.3%, proving that R-SMILES helps the model focus on the more meaningful differences between the input and output SMILES.

For other top-K accuracies, results for both indicators are similar and can be found in Fig. S2. These results all demonstrate the effectiveness and robustness of R-SMILES.

**Multistep retrosynthesis prediction by our method.** By applying our template-free variant recursively, we verify our method with several multistep retrosynthesis examples reported in the literature, including febuxostat [35], salmeterol [36], an allosteric activator for GPX<sub>4</sub> [16], and a 5-HT<sub>6</sub> receptor ligand [37]. As shown in Fig. 5, our method successfully predicts the complete synthetic pathway for these examples.

Febuxostat (Fig. 5a) is a novel anti-gout drug as the non-purine selective inhibitor of xanthine oxidase. Cao et al. [35] reported a new reaction pathway for it based on the Suzuki cross-coupling reaction in 2016. Our predicted first step is hydrolysis of the ester, which is exactly the same as reported. For the remaining reaction steps, our method provides two different synthetic routes. The first one is the same as reported, where 3-cyano-4-isobutoxyphenyl boronic acid and ethyl 2-bromo-4-methylthiazole-5-carboxylate are taken as the reactants of the Suzuki cross-coupling reaction. However, the second one reports nucleophilic substitution to get aryl boronic esters for the Suzuki cross-coupling reaction. As illustrated by Urawa et al. [38], the utilization of aryl boronic esters is usually accompanied by



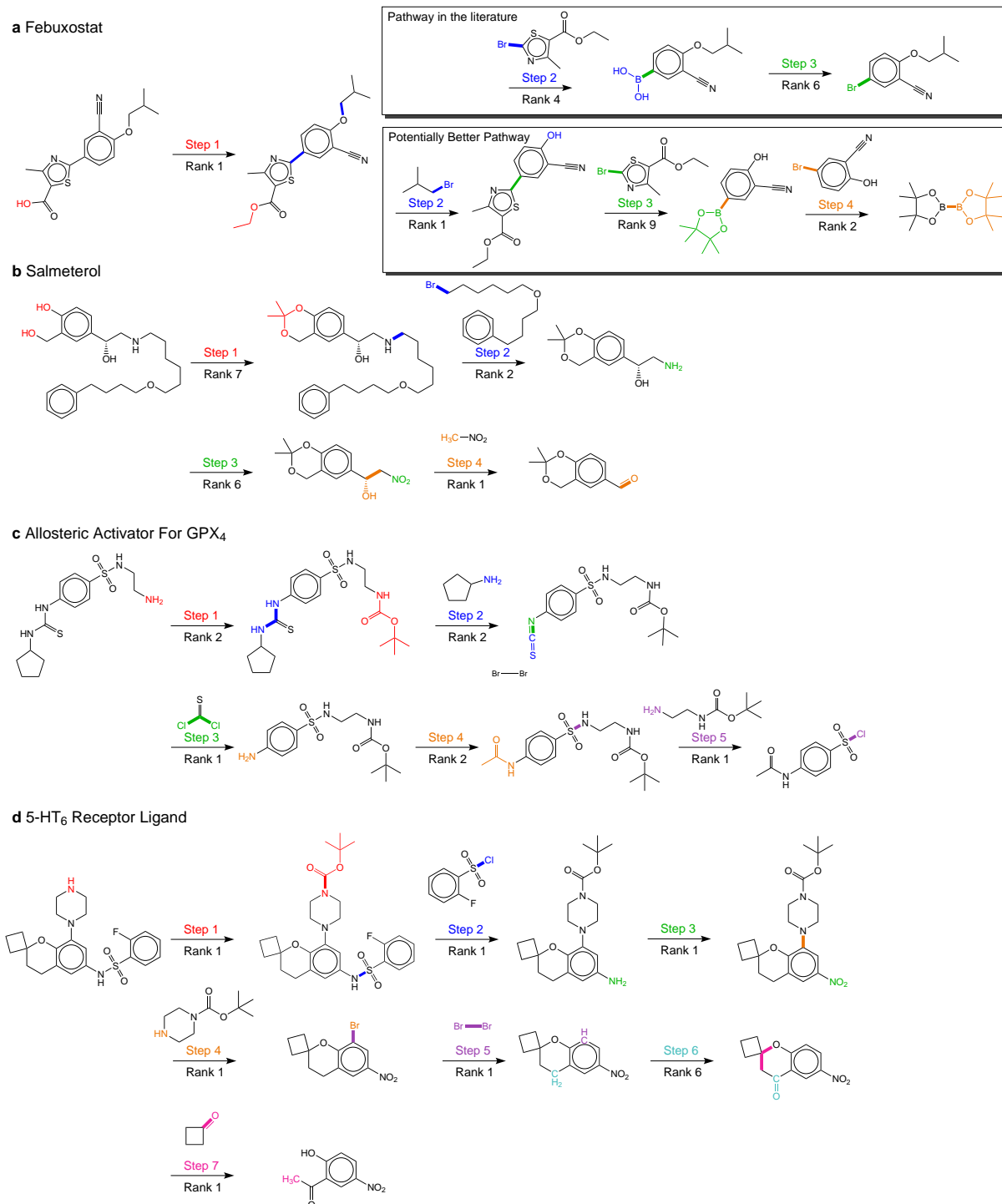


**Fig. 5 Multistep retrosynthesis predictions by our method.** **a**, febuxostat, **b**, salmeterol, **c**, an allosteric activator for GPX<sub>4</sub>, **d**, a 5-HT<sub>6</sub> receptor ligand. The reaction centers and transformations from products to reactants are highlighted in different colors at different reaction steps. In addition to the reaction pathway in the literature, we report a potentially better reaction pathway for febuxostat.

higher yields than aryl boronic acid, which suggests that the second one may be more consistent with experimental experience. The final steps of them both involve borylation, where the second one is reported by Ishiyama et al. [39]. Therefore, we believe that our method suggests a potentially better synthetic pathway for febuxostat.

Salmeterol (Fig. 5b) is a potent, long-acting,  $\beta$ 2-adrenoreceptor agonist. Guo et al. [36] proposed a reaction pathway for it based on the asymmetric Henry reaction. Although the first three steps provided by our method do not exist in the literature, they are all explainable. The first step reports the hydrolysis of cyclic acetal, where cyclic acetal has been proved to be stable. Considering the high activity of the phenolic hydroxyl group and the hydroxyl group connected to the benzyl group, the formation of cyclic acetal can effectively prevent the occurrence of side reactions, which illustrates the model has distinguished the properties of protection groups and preserved it to the starting compound. The second step involves the amination of halohydrocarbon, and the third step involves the reduction of the nitro group. The final step, which is the core reaction, is the asymmetric Henry reaction, where our method has successfully reproduced the generation of new chiral centers at the rank-1 prediction. This result also matches our conclusion of the great performance involving chirality as mentioned above.

The synthetic pathway of the GPX<sub>4</sub> activator compound (Fig. 5c) is reported by Lin et al. [16], who predicted the synthetic pathway with a template-free model by enumerating different reaction types. However, even without the reaction type, our method succeeds for all five reaction steps within the top-2 predictions, which directly demonstrates the superiority of our method. Among five reaction steps, the Hinsberg reaction of the final step is the core reaction of the whole synthetic pathway, where our method succeeds at the rank-1 prediction.

Nirogi et al. [37] proposed a benzopyran sulfonamide derivative as an antagonist of 5-HT<sub>6</sub> receptor (Fig. 5d) in 2015. Although the synthetic pathway consists of seven reaction steps, our method succeeds at the rank-1 prediction for all steps except the sixth one that is predicted at the rank-6 prediction. The second and fourth steps

have attracted our attention, which are the Hinsberg reaction and Nucleophilic Aromatic Substitution reaction (SNAr). In the Hinsberg reaction, primary amines are able to react with benzenesulfonyl chloride. In SNAr, meta-nitro group reduces the density of electron cloud, which is conducive to the occurrence of reaction. The success of key steps in the long synthetic pathway further demonstrates the robustness of our method.

For all 22 reactions in these four examples, our method succeeds at the top-10 predictions, and mostly at the top-2 predictions. In addition, our method proposes a novel synthetic pathway for febuxostat that is more consistent with experimental experience. These exciting results all demonstrate the great potential of our method for multistep retrosynthesis.

## Conclusion

In this article, we propose R-SMILES for retrosynthesis. Unlike canonical SMILES that is widely adopted in the current literature, R-SMILES specifies a tightly aligned one-to-one mapping between the input and output SMILES, which decreases the edit distance significantly. With R-SMILES, the retrosynthesis model is largely relaxed from learning the complex syntax and can be dedicated to learning the chemical knowledge for retrosynthesis. We implement both template-free and semi-template models to validate the proposed R-SMILES, both yielding superiority performance to state-of-the-art methods. To better understand the proposed method, we further provide several interesting discussions, *e.g.*, the visualization of the cross-attention between input and output tokens. Finally, the synthetic pathways of some organic compounds are provided to showcase the effectiveness of the proposed method.

Albeit striking performance achieved in retrosynthesis, we believe that the potential of R-SMILES is not fully explored in this work. One promising application scenario is forward reaction prediction, where the proposed R-SMILES may facilitate the model learning in a similar way to retrosynthesis. Another possible scenario is reaction type classification, where the reaction center can be easier to be identified with the proposed R-SMILES as inputs for reactants and products.

## Method

**Root-aligned SMILES.** First of all, we follow Schwaller et al.’s [40] regular expression to tokenize SMILES to meaningful tokens. To get R-SMILES, we have to find the common structures of the source and the target, which can be found by atom mapping or substructure matching algorithms [41]. In this work, we use atom mapping in the reactions to find the common structures.

The root alignment operation is effortless in the P2R stage, where the input is only a single product. We can select a root atom from the product randomly first, and set it as the root atom to obtain the product SMILES. According to the new order of product tokens, we can find each corresponding root atom for reactants. We remove all atom mapping from the final input and output to avoid any information leak. An example of the root alignment is shown in Table S3. In the S2R stage, we put the product and synthon SMILES together as input, separated by a special token that does not exist in the SMILES syntax. We choose to align reactants to synthons to minimize the difference between the input and the output since there is a one-to-one mapping between synthons and reactants. The product is aligned to the largest synthon (*i.e.*, the synthon with the most atoms). Taking the reaction in Table S3 as the example, we can get the synthon SMILES with atom-mapping first, which is “[C:1]([CH:2]=[CH2:3])=[O:4].[O:5][CH2:6][C:7].[Cl:8])([Cl:9])[Cl:10]”. By selecting [Cl:8] and [C:1] as the roots of the synthons, we can obtain the input as “Cl C ( Cl ) ( Cl ) C O C ( = O ) C = C <split> Cl C ( Cl ) ( Cl ) C O . C ( = O ) C = C” and the output as “Cl C ( Cl ) ( Cl ) C O . C ( = O ) ( Cl ) C = C”. After root alignment, the input and output are highly similar to each other, which helps the model to reduce the search space and makes cross-attention stronger.

**Vanilla transformer.** We take the vanilla transformer as the backbone of our autoencoder. Vanilla transformer [34] is an end-to-end model following a stepwise and autoregressive encoder-decoder fashion. Taken the product SMILES  $X = (x_0, x_1, x_2, \dots, x_n)$  and partially decoded reactant SMILES  $Y = (y_0, y_1, y_2, \dots, y_j)$  as the input, it is trained to predict the next token of reactant SMILES  $y_{j+1}$ . The key idea of the vanilla transformer is the attention mechanism, which allows

each token to capture the global information and is quite suitable for SMILES representations. The encoder and decoder are both composed of multiple stacked multihead attention layers consisting of a multihead attention module and a position-wise feed forward module.

Before passing into the encoder, SMILES tokens are embedded to continuous vector representations  $X' = (x'_0, x'_1, x'_2, \dots, x'_n)$ . The multihead attention module consists of multiple scaled-dot product layers that run in parallel. A single scaled-dot product calculation works as follows:

$$\begin{aligned} \text{Attention}(Q, K, V) &= \text{softmax}\left(\frac{QK^T}{\sqrt{d_k}}\right)V \\ Q &= W_Q X' \\ K &= W_K X' \\ V &= W_V X' \end{aligned} \quad (1)$$

where  $Q$ ,  $K$ ,  $V$  represent query, key, value matrix, respectively;  $W_Q$ ,  $W_K$ ,  $W_V$  are all trainable parameters;  $d_k$  means the dimension of  $K$ . Depending on where  $Q$ ,  $K$ ,  $V$  come from, multihead attention can be the self-attention mechanism or cross-attention mechanism. After the attention calculation of each head, they can be concatenated as follows:

$$\begin{aligned} Z &= \text{Concat}(h_0, h_1, \dots)W^0 \\ h_i &= \text{Attention}(Q_i, K_i, V_i) \end{aligned} \quad (2)$$

The position-wise feed forward module is a simple fully connected layer that utilizes the concept of residual block and works as follows:

$$\text{FFN}(Z) = \max(0, W_1 z + b_1)W_2 + b_2 \quad (3)$$

After the calculation of feed forward module, updated token vectors can be passed to another multihead attention layer. We use the vanilla transformer architecture composed of 6 layers for both encoder and decoder with 8 attention heads for all experiments.

During the inference stage, the transformer takes the product SMILES and decoded reactant as the input to predict the probability of the next reactant SMILES token, which can be represented by a conditional probability distribution:

$$p(y|X) = \prod_{i=1}^m p(y_i|y_{<i}, X) \quad (4)$$

where  $m$  is the maximum number of reactant tokens. The “bos” (begin of sentence) token is the beginning of reactant tokens. When the last predicted token is “eos” (end of sentence), the decoding process completes.

**Data augmentation with R-SMILES.** We successively perform data augmentation and root alignment on the training data, and only perform data augmentation on the test data. When inferring on the valid and test data, we input multiple SMILES of a molecule respectively and get multiple sets of outputs correspondingly. After removing error SMILES that cannot be recognized by Rdkit [42] and converting all outputs to canonical SMILES, we refer to Tekto et al.’s approach [19] that scores these outputs uniformly as follows:

$$score(output) = \sum_{n=1}^{aug. beam} \sum_{i=1}^{beam} \frac{1}{1 + 0.001 * (i - 1)} \quad (5)$$

where *aug.* represents the augmentation times of the test set, and *beam* represents the beam size. After scoring uniformly, we can select outputs with top-K scores as the final result.

**Mixed loss for the P2S stage** Because the P2S stage is more suitable to be formulated as a link prediction problem, we use a graph model during the P2S stage. To get our backbone graph module, we add information propagation mechanism of edges to RGCN [25]. We use a 6-layer of the graph module to build our graph model. Then we propose the loss function from the perspective of the graph, the atom, and the bond to train the graph model. In addition to judging whether each bond is broken, we additionally judge the number of broken bonds on each graph and whether the atoms are connected to the broken bonds. The former helps us judge the number of reaction centers on each graph, and the latter can be used as an auxiliary task to identify the reaction centers. We give each edge a probability to break. According to the predicted number of the broken edges, select the edges with the highest probabilities to get rid of setting the threshold of the broken probability.

**Training settings.** We split USPTO-50K dataset randomly into train, valid and test sets with the

8:1:1 ratio. As for the USPTO-FULL dataset, we use the same data split as Dai et al. [9]. During the pretraining stage, products in the training set of USPTO-FULL are used for self-supervised training, where products in the test set of USPTO-50K are removed. We apply 20× augmentation at training and test sets of USPTO-50K, and 5× augmentation at training and test sets of USPTO-FULL, respectively. For sequence-based models, we set the hidden size as 256 except that the dimension of  $Q$ ,  $K$ ,  $V$  is 64. We also use the Adam optimizer and a varied learning rate with 8,000 warm up steps. The input and output share the same vocabulary, but their embedding layers are separated. The maximum sentence length is 500 and 1000 for USPTO-50K and USPTO-FULL, respectively. For graph-based models, we assign the same weights to all three losses and set the hidden size as 128. We use the Adam optimizer with fixed learning rates for training. Learning rates of 0.001 and 0.0001 are used for USPTO-50K and USPTO-FULL, respectively. The more detailed settings can be found in our code repository.

## Data availability

USPTO-50K dataset was obtained from the Github reported by Coley et al.[7](<https://github.com/connorcoley/retrosim>). USPTO-Full dataset was obtained from the study reported by Dai et al.[9](<https://github.com/Hanjun-Dai/GLN>).

## Code availability

The code used in the study is publicly available from the GitHub repository: <https://github.com/otori-bird/retrosynthesis>.

## References

- [1] Corey, E. J. Robert robinson lecture. retrosynthetic thinking—essentials and examples. *Chemical society reviews* **17**, 111–133 (1988).
- [2] Corey, E. J. The logic of chemical synthesis: multistep synthesis of complex carbonic molecules (nobel lecture). *Angewandte Chemie International Edition in English* **30** (5), 455–465 (1991).

- [3] Pensak, D. A. & Corey, E. J. Lhasa—logic and heuristics applied to synthetic analysis. In (ACS Publications, 1977).
- [4] Johnson, P. *et al.* Designing an expert system for organic synthesis in expert systems application in chemistry. In *ACS Symposium Series of American Chemical Society* (1989).
- [5] Gasteiger, J. *et al.* Computer-assisted synthesis and reaction planning in combinatorial chemistry. *Perspectives in Drug Discovery and Design* **20** (1), 245–264 (2000).
- [6] Szymkuć, S. *et al.* Computer-assisted synthetic planning: the end of the beginning. *Angewandte Chemie International Edition* **55** (20), 5904–5937 (2016).
- [7] Coley, C. W., Rogers, L., Green, W. H. & Jensen, K. F. Computer-assisted retrosynthesis based on molecular similarity. *ACS central science* **3** (12), 1237–1245 (2017).
- [8] Segler, M. H. & Waller, M. P. Neural-symbolic machine learning for retrosynthesis and reaction prediction. *Chemistry—A European Journal* **23** (25), 5966–5971 (2017).
- [9] Dai, H., Li, C., Coley, C., Dai, B. & Song, L. Retrosynthesis prediction with conditional graph logic network. *Advances in Neural Information Processing Systems* **32**, 8872–8882 (2019).
- [10] Chen, S. & Jung, Y. Deep retrosynthetic reaction prediction using local reactivity and global attention. *JACS Au* **1** (10), 1612–1620 (2021).
- [11] Guo, Z., Wu, S., Ohno, M. & Yoshida, R. Bayesian algorithm for retrosynthesis. *Journal of Chemical Information and Modeling* **60** (10), 4474–4486 (2020).
- [12] Lee, H. *et al.* Retcl: A selection-based approach for retrosynthesis via contrastive learning. Preprint at <https://arxiv.org/abs/2105.00795> (2021).
- [13] Liu, B. *et al.* Retrosynthetic reaction prediction using neural sequence-to-sequence models. *ACS central science* **3** (10), 1103–1113 (2017).
- [14] Karpov, P., Godin, G. & Tetko, I. V. A transformer model for retrosynthesis. In *International Conference on Artificial Neural Networks* 817–830 (Springer, 2019).
- [15] Zheng, S., Rao, J., Zhang, Z., Xu, J. & Yang, Y. Predicting retrosynthetic reactions using self-corrected transformer neural networks. *Journal of Chemical Information and Modeling* **60** (1), 47–55 (2019).
- [16] Lin, K., Xu, Y., Pei, J. & Lai, L. Automatic retrosynthetic route planning using template-free models. *Chemical science* **11** (12), 3355–3364 (2020).
- [17] Yan, C. *et al.* Retroxpert: Decompose retrosynthesis prediction like a chemist. *Advances in Neural Information Processing Systems* **33**, 11248–11258 (2020).
- [18] Wang, X. *et al.* Retroprime: A diverse, plausible and transformer-based method for single-step retrosynthesis predictions. *Chemical Engineering Journal* **420**, 129845 (2021).
- [19] Tetko, I. V., Karpov, P., Van Deursen, R. & Godin, G. State-of-the-art augmented nlp transformer models for direct and single-step retrosynthesis. *Nature communications* **11** (1), 1–11 (2020).
- [20] Seo, S.-W. *et al.* Gta: Graph truncated attention for retrosynthesis. *Proceedings of the AAAI Conference on Artificial Intelligence* **35** (1), 531–539 (2021).
- [21] Kim, E., Lee, D., Kwon, Y., Park, M. S. & Choi, Y.-S. Valid, plausible, and diverse retrosynthesis using tied two-way transformers with latent variables. *Journal of Chemical Information and Modeling* **61** (1), 123–133 (2021).
- [22] Shi, C., Xu, M., Guo, H., Zhang, M. & Tang, J. A graph to graphs framework for retrosynthesis prediction. In *International*

- Conference on Machine Learning* 8818–8827 (PMLR, 2020).
- [23] Somnath, V. R., Bunne, C., Coley, C. W., Krause, A. & Barzilay, R. Learning graph models for retrosynthesis prediction. In *Thirty-Fifth Conference on Neural Information Processing Systems* (2021).
- [24] Sacha, M. *et al.* Molecule edit graph attention network: modeling chemical reactions as sequences of graph edits. *Journal of Chemical Information and Modeling* **61** (7), 3273–3284 (2021).
- [25] Schlichtkrull, M. *et al.* Modeling relational data with graph convolutional networks. In *European semantic web conference* 593–607 (Springer, 2018).
- [26] Velickovic, P. *et al.* Graph attention networks. *stat* **1050**, 20 (2017). Preprint at <https://arxiv.org/abs/1710.10903>.
- [27] Weininger, D. Smiles, a chemical language and information system. 1. introduction to methodology and encoding rules. *Journal of chemical information and computer sciences* **28** (1), 31–36 (1988).
- [28] O’Boyle, N. M. Towards a universal smiles representation—a standard method to generate canonical smiles based on the inchi. *Journal of cheminformatics* **4** (1), 1–14 (2012).
- [29] Schneider, N., Sayle, R. A. & Landrum, G. A. Get your atoms in order — an open-source implementation of a novel and robust molecular canonicalization algorithm. *Journal of chemical information and modeling* **55** (10), 2111–2120 (2015).
- [30] Pu, Y. *et al.* Variational autoencoder for deep learning of images, labels and captions. *Advances in neural information processing systems* **29** (2016).
- [31] He, K. *et al.* Masked autoencoders are scalable vision learners. Preprint at <https://arxiv.org/abs/2111.06377> (2021).
- [32] Sun, R., Dai, H., Li, L., Kearnes, S. & Dai, B. Towards understanding retrosynthesis by energy-based models. *Advances in Neural Information Processing Systems* **34** (2021).
- [33] Schneider, N., Stiefl, N. & Landrum, G. A. What’s what: The (nearly) definitive guide to reaction role assignment. *Journal of chemical information and modeling* **56** (12), 2336–2346 (2016).
- [34] Vaswani, A. *et al.* Attention is all you need. In *Advances in Neural Information Processing Systems* (Curran Associates, Inc., 2017).
- [35] Cao, Q. M., Ma, X. L., Xiong, J. M., Guo, P. & Chao, J. P. The preparation of febuxostat by suzuki reaction. *Chinese Journal of New Drugs* (2016).
- [36] Guo, Z.-L., Deng, Y.-Q., Zhong, S. & Lu, G. Enantioselective synthesis of (r)-salmeterol employing an asymmetric henry reaction as the key step. *Tetrahedron: Asymmetry* **22** (13), 1395–1399 (2011).
- [37] Nirogi, R. V., Badange, R., Reballi, V. & Khagga, M. Design, synthesis and biological evaluation of novel benzopyran sulfonamide derivatives as 5-HT<sub>6</sub> receptor ligands. *Asian Journal of Chemistry* **27** (6), 2117 (2015).
- [38] Urawa, Y., Naka, H., Miyazawa, M., Souda, S. & Ogura, K. Investigations into the suzuki-miyaura coupling aiming at multikilogram synthesis of e2040 using (o-cyanophenyl) boronic esters. *Journal of organometallic chemistry* **653** (1-2), 269–278 (2002).
- [39] Ishiyama, T., Murata, M. & Miyaura, N. Palladium (0)-catalyzed cross-coupling reaction of alkoxydiboron with haloarenes: a direct procedure for arylboronic esters. *The Journal of Organic Chemistry* **60** (23), 7508–7510 (1995).

- [40] Schwaller, P., Gaudin, T., Lanyi, D., Bekas, C. & Laino, T. “found in translation”: predicting outcomes of complex organic chemistry reactions using neural sequence-to-sequence models. *Chemical science* **9** (28), 6091–6098 (2018).
- [41] Englert, P. & Kovács, P. Efficient heuristics for maximum common substructure search. *Journal of chemical information and modeling* **55** (5), 941–955 (2015).
- [42] Landrum, G. Rdkit: Open-source cheminformatics software .

# Supplementary Information: Root-aligned SMILES for Molecular Retrosynthesis Prediction

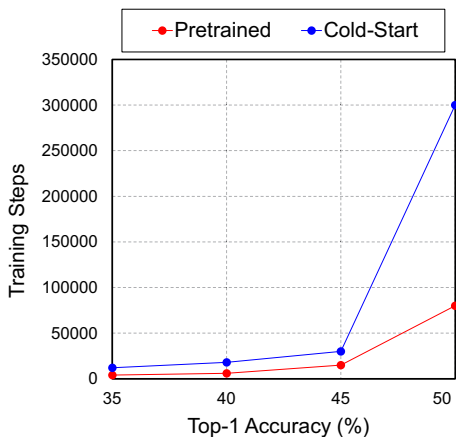


**Fig. S1 Training steps with/without the pre-trained model on USPTO-50K for the P2R stage.** The training set of USPTO-50K is applied 20 $\times$  augmentation.

## S1 Analysis of Pretrained Autoencoder

We used a similar approach to the masked language model of BERT [1] for pretraining. Specifically, 15% of tokens in SMILES are masked. Every masked token has an 80% probability of being replaced with the “unknown” token, a 10% probability of being replaced with any token in the vocabulary, and keeps unchanged for the rest of the cases. After pretraining, we can see in Fig. S1 that the training time has been dramatically reduced, which helps a lot in the case of very limited computational resources.

## S2 Comparisons of P2S and S2R accuracy

We report the performances of our methods for P2S and S2R stages besides others in Table S1.

**Table S1 Comparisons of top-K accuracy in P2S and S2R stages on USPTO-50K**

Stage	Model	top-K Accuracy(%)			
		K=1	3	5	10
P2S	G2Gs [2]	75.8	83.9	85.3	85.6
	RetroXpert [3]	59.9	-	-	-
	GraphRetro [4]	70.8	92.2	93.7	94.5
	RetroPrime [5]	65.6	87.7	92.0	-
	Ours (edge)	79.5	-	-	-
	Ours (edge + node)	78.0	-	-	-
	Ours (edge + graph)	79.8	87.5	88.2	88.6
	Ours (edge + node + graph)	<b>82.0</b>	88.7	89.2	89.5
	Ours (R-SMILES)	73.4	<b>94.2</b>	<b>97.9</b>	<b>99.1</b>
S2R	G2Gs [2]	61.1	81.5	86.7	90.0
	GraphRetro [4]	<b>75.6</b>	87.7	92.9	96.3
	RetroPrime [5]	73.4	87.9	89.8	90.4
	Ours (R-SMILES)	73.9	<b>91.9</b>	<b>95.2</b>	<b>97.4</b>

*edge, node, graph*: edge, node, graph loss, respectively. *all*: all the losses are used. *R-SMILES*: root-aligned SMILES.

For the P2S stage, our graph-based method that is taken as a component of our semi-template method achieves the best top-1 exact match accuracy, surpassing the current SOTA with the 6.2% margin. Compared with graph-based methods that formulate the P2S stage as a link prediction problem, sequence-based methods formulate it as a seq2seq task from scratch, which turns out to be an inborn disadvantage. But despite this, our sequence-based method still outperforms others at all top-K accuracies with the exception of top-1, where the top-10 accuracy has even been improved from 94.5% of the baseline to 99.1%. For the S2R stage, our method also achieves the best results with the exception of only top-1. Compared with another sequence-based method RetroPrime [5], our method outperforms it for all metrics both in P2S and S2R stages.



Table S2 Edit distance with/without R-SMILES

dataset	data size	length		unique characters	edit Distance	
		Pro.	Rea.		Cano.	R-SMILES
USPTO50K <sup>×1</sup>	50,016	43.4	47.4	8.4	17.9	14.1 (-21%)
USPTO50K <sup>×5</sup>	250,060	45.1	49.6	9.1	28.4	14.1 (-50%)
USPTO50K <sup>×20</sup>	1,000,240	45.4	50.0	9.4	30.2	14.1 (-53%)
USPTO-Full-cleaned <sup>×1</sup>	960,198	41.4	48.1	10.9	19.8	16.6 (-16%)
USPTO-Full-cleaned <sup>×5</sup>	4,800,990	43.1	50.4	12.3	29.2	16.6 (-43%)

Canonical SMILES is always included in the datasets without R-SMILES. Except for the data size, all data are shown on average. Dataset<sup>×*m*</sup>: *m* times data augmentation. Pro.: product SMILES. Rea.: reactant SMILES. unique characters: the characters only appear in reactant SMILES or product SMILES. Cano.: canonical and randomized SMILES. R-SMILES.: root-aligned SMILES.

Table S3 An example (US20020192594A1 in USPTO-50K) of performing root alignment

Step	reactant >> product
(1) Original data	Cl[C:1]([CH:2]=[CH2:3])=[O:4].[OH:5][CH2:6][C:7]([Cl:8])([Cl:9])[Cl:10] >>[C:1]([CH:2]=[CH2:3])(=[O:4])[O:5][CH2:6][C:7]([Cl:8])([Cl:9])[Cl:10]
(2) Randomly select a root atom from the product	[C:1]([CH:2]=[CH2:3])(=[O:4])[O:5][CH2:6][C:7]([Cl:8])([Cl:9])[Cl:10]
(3) Product R-SMILES with root atom mapping	[Cl:8][C:7]([Cl:9])([Cl:10])[C:6][O:5][C:1](=[O:4])[C:2]=[C:3]
(4) Atom-mapping removal	C1C(Cl)(Cl)COC(=O)C=C
(5) Select reactant roots according to the product	Cl[C:1]([CH:2]=[CH2:3])=[O:4].[OH:5][CH2:6][C:7]([Cl:8])([Cl:9])[Cl:10]
(6) Reactant R-SMILES without atom mapping	C1C(Cl)(Cl)CO.C(=O)(Cl)C=C
(7) Tokenization	
Input	C1 C ( Cl ) ( Cl ) C O C ( = O ) C = C
Output	C1 C ( Cl ) ( Cl ) C O . C ( = O ) ( Cl ) C = C

The root atoms are bold. (1) Select a reaction from the dataset. (2) Randomly select an atom as the root atom. In this case, [Cl:8] is selected. (3) Obtain the product R-SMILES with specified root atom. (4) Remove the atom mapping to get the final input. (5) From the left to the right of the reactant SMILES, look for the atom mapping that appeared on the product SMILES. Once found, the atom is selected as the root of the reactant. In this case, [C:1] and [Cl:8] are selected. (6) Obtain the reactant R-SMILES without atom mapping to get the final output. (7) Tokenize the SMILES.

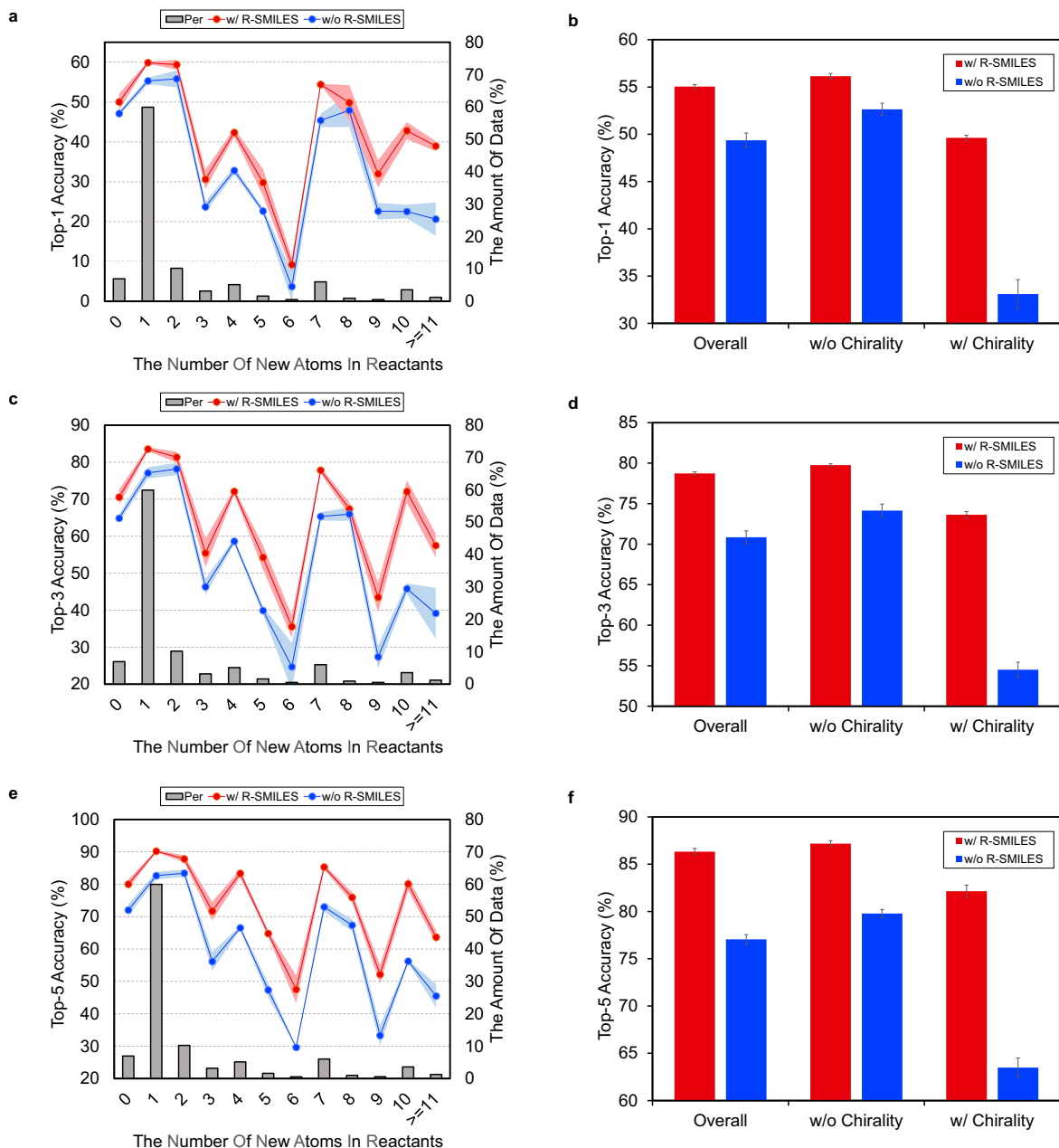


**Fig. S2 Extra top-K accuracy (%) for complex reactions.** **a, c, e**, Top-1, top-3, and top-5 accuracies according to the number of new atoms in reactants. The red and blue lines represent the performance with/without R-SMILES. The gray bar means the percentage of this kind of reaction in the test set. **b, d, f**, Top-1, top-3, and top-5 accuracies for reactions involving with or without chirality. The red and blue bars represent the performance with or without R-SMILES.

## References

- [1] Devlin, J., Chang, M.-W., Lee, K. & Toutanova, K. Bert: Pre-training of deep bidirectional transformers for language understanding. Preprint at <https://arxiv.org/abs/1810.04805> (2018).
- [2] Shi, C., Xu, M., Guo, H., Zhang, M. & Tang, J. A graph to graphs framework for retrosynthesis prediction. In *International Conference on Machine Learning* 8818–8827 (PMLR, 2020).
- [3] Yan, C. *et al.* Retroxpert: Decompose retrosynthesis prediction like a chemist. *Advances in Neural Information Processing Systems* **33**, 11248–11258 (2020).
- [4] Somnath, V. R., Bunne, C., Coley, C. W., Krause, A. & Barzilay, R. Learning graph models for retrosynthesis prediction. In *Thirty-Fifth Conference on Neural Information Processing Systems* (2021).
- [5] Wang, X. *et al.* Retroprime: A diverse, plausible and transformer-based method for single-step retrosynthesis predictions. *Chemical Engineering Journal* **420**, 129845 (2021).